Superhydrophobicity: Localized Parameters and Gradient Surfaces

G. McHale*, S. J. Elliott, M. I. Newton and N. J. Shirtcliffe
School of Science and Technology, Nottingham Trent University
Clifton Lane, Nottingham NG11 8NS, UK

Abstract

The use of Cassie and Baxter's equation and that of Wenzel have been subject to some criticism of late. It has been suggested that researchers use these equations without always considering the assumptions that have been made and sometimes apply them to cases that are not suitable. This debate has prompted a reconsideration of the derivation of these equations using the concept of parameters for the Wenzel roughness and Cassie-Baxter solid surface fractions that are local to the three-phase contact lines. In such circumstances, we show the roughness and Cassie-Baxter solid fractions depend not only on the substrate material, but also on which part of the substrate is being sampled by the three-phase contact lines of a given droplet. We show that this is not simply a theoretical debate, but is one which has direct consequences for experiments on surfaces where the roughness or spatial pattern varies across the surface. We use the approach to derive formulae for the contact angle observed on a double length scale surface under the assumption that the small-scale features on the peaks of larger scale features are either wetted or non-wetted. We also discuss the case of curved and re-entrant surface features and how these bring the Young's law contact angle into the formula for roughness and the condition for suspending droplets without penetration into the surface. To illustrate the use of local parameters, we consider the case of a variation in Cassie-Baxter fraction across a surface possessing a homogeneous hydrophobic surface chemistry and discuss the conditions (droplet volume, surface hydrophobicity, gradient in superhydrophobicity and contact angle hysteresis) under which a droplet may be set into motion. We show that different contact angles on each side of a droplet of water placed on such a surface can generate sufficient lateral force for the droplet to move towards the region of the surface with the lowest contact angle. Using an electrodeposited copper surface with a radial gradient in superhydrophobicity we exemplify these ideas by showing experimentally that droplets enter into self-actuated motion and accumulate in the centre of the surface where the wettability is higher. In principle, paths can be defined and water droplets can be collected by creating such gradients in superhydrophobicity through changes in the lateral topography of the surface.

Keywords Superhydrophobicity, Cassie-Baxter, Wenzel, Wetting, Contact Angle

* To whom correspondence should be addressed.
Tel: +44 115 8483383; email: glen.mchale@ntu.ac.uk.

1. Introduction

Superhydrophobic surfaces constitute one class of wetting problems in which topography amplifies the effect of surface chemistry [1]. In the superhydrophobic case, water repellence is emphasized to create extremely high contact angles and low contact angle hysteresis. Surfaces with high contact angles and high contact angle hysteresis, and surfaces that create superspreading [2,3], superwetting or hemiwicking [4, 5] use similar topographic principles, but these latter surfaces emphasize the spreading tendency of a liquid on a given substrate material. Many methods exist for creating superhydrophobic surfaces and these have been reviewed by a range of authors [6-9]. It is often the case that their properties are discussed with reference to the Cassie-Baxter and Wenzel models [10-13] and, in particular, with reference to a very specific type of surface composed of flat-topped vertical posts [14]. This has led to a common description of superhydrophobicity as due to a droplet behaving as if it were sitting on a bed-of-nails (a fakir's carpet). Whilst it is certainly true that a droplet is supported by the surface protrusions below the entirety of the solid surface within the wetted perimeter of a droplet, this simplified view appears to have caused confusion with regards to the definition of the Cassie-Baxter solid fraction and Wenzel roughness parameter [15-17]. With the maturing of the field of superhydrophobicity, such that many materials and methods are now available to create surfaces, it is important that topographic amplification of wetting occurring locally at the three-phase contact lines, both at the perimeter of the droplet and below the droplet within that perimeter, are understood. One potential area of application for superhydrophobic surfaces is droplet transport and here well-developed concepts of wettability gradients and actuating forces are required [18, 19].

In Section 2, wetting on defect and composite surfaces is discussed and this leads on, in Section 3, to a consideration of the implications for understanding the Wenzel and Cassie-Baxter models. The principal outcome is to emphasize that the Cassie-Baxter fraction and Wenzel roughness parameter are defined locally to the three-phase contact lines [16]; similarly the relevant Young's law contact angle in these two formulae relate to the local surface chemistry. In Section 4, we discuss a number of more complex cases, including two-length scales, re-entrant surfaces and wetting on spherical beads; spherical beads provide an example of a system for which roughness may become a function of the Young's law contact angle. In Section 5, we consider how varying the wettability across a surface by changing the Cassie-Baxter fraction with position might be used to generate motion of droplets. Finally, in Section 6, we exemplify some of these ideas by briefly presenting an example of a surface where we created a radial gradient in superhydrophobicity using electrodeposition of copper so that droplets roll to a central location. Furthermore, we suggest that more complex patterns could be used to define paths and tracks for droplet transport [1, 16].

2. Wetting on Defect and Composite Surfaces

A fundamental question in wetting is whether processes are local to the three-phase contact lines or whether the entireties of the various interfaces need to be taken into account. First consider measuring advancing and receding contact angles by using a syringe inserted into the apex of a sessile droplet. This causes a slight distortion of the liquid-vapor interface and so prevents axisymmetric drop shape analysis based on the full profile of the droplet. An alternative method, used in studies of possible line tension effects [20, 21], is to fill the droplet by delivering liquid through a hole in the substrate (fig. 1a). However, the existence of the hole now means the droplet sits on a composite surface of the solid substrate and a central area which is the liquid-filled hole. The presumption is that provided the droplet contact area is wider than the hole, this does not alter the contact angles measured at the perimeter of the droplet. Now imagine that as the droplet grows in volume it encounters successive changes in surface chemistry from one with a low contact angle to one with a higher contact angle, i.e. a surface with radial rings of differing surface chemistry. This experiment has been reported in the literature (e.g. [22]) and the contact angles measured, both advancing and receding, are those that would be expected for a droplet entirely on a surface with the same surface chemistry as that surface chemistry where the perimeter rests upon [23, 24]. Our expectation is that when the droplet perimeter reaches the boundary from a lower contact angle to higher contact angle ring, the droplet perimeter will stop advancing and the contact angle will increase until suddenly a rapid advance will occur across part of the

higher contact angle ring (see also ref. [22]). From these considerations it should, therefore, be clear that contact angles are local to the three-phase contact lines; this is a long held view within the literature on contact angles (see ref [25]). The phrase "three-phase contact lines" has been chosen carefully to be plural to emphasize that there may be more than one such three-phase contact line for a droplet. For example, if in fig. 1 the tube feeding liquid into the droplet from below was empty of liquid, but was narrow enough and sufficiently hydrophobic that liquid from the droplet did not penetrate into it, then a three-phase contact line would exist below the droplet; this would be an additional three-phase contact line disconnected from the one at the droplet's external perimeter on the substrate.

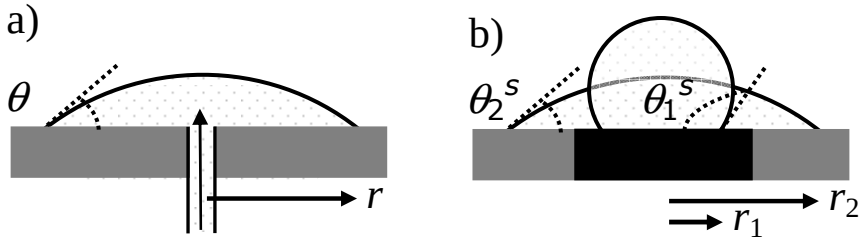

Figure 1. a) Measurement of advancing contact angle, θ, for a droplet on a smooth flat surface (r is the droplet contact radius), and b) two equilibrium configurations for a droplet of a fixed volume on a smooth flat hydrophilic surface characterized by a Young's law contact angle θ_2^S, with a central hydrophobic defect characterized by a Young's law contact angle θ_1^S (r_1 and r_2 are the droplet contact radii for the two droplet configurations).

Now consider a circular hydrophobic defect with, say, $\theta_1^s = 110^o$, within a more hydrophilic region having, say, $\theta_2^s = 70^o$, where both contact angles are due to a homogeneous surface chemistry within their respective regions. For a given volume of droplet, the total surface free energy can be calculated. For some volumes, such as $V=1\times10^{-9}$ m^3, we find that provided the central defect is within a certain size range, two stable configurations that satisfy a minimum in the surface free energy can exist [16]. The first of these is with a droplet sitting entirely on the hydrophobic defect and the second is with the droplet perimeter sitting entirely on the more hydrophilic region. Thus, not only is the Young's law contact angle local to the three-phase contact line important, but the initial state is also important because it will determine what configurations close to that initial state can be sampled by the three- phase contact line to reach an equilibrium.

3. Wenzel and Cassie-Baxter Equations with Local Parameters

We now consider the analogous situation of a rough defect within a smooth surface area with a droplet sitting entirely on the defect and maintaining contact with the surface at all points beneath itself (fig. 2a). The contact angle, θ_W, for this situation is described by the Wenzel equation [8],

$$\cos\theta_W = r\cos\theta_e \tag{1}$$

where θ_e is the Young's law contact angle and r is the Wenzel roughness factor, which is often defined to be the ratio of actual area to planar projection of area of the substrate. This implies that roughness is a property of the substrate alone, which is clearly not the case, since that would then imply that the extent of smooth area completely remote from the vicinity of the droplet would determine the roughness factor. Restricting the definition to the area beneath the droplet would give a definition $r=A_{wetted}/\pi r_c^2$ where r_c is the planar contact radius. However, this then produces a definition that seems contradictory to the situation discussed for a single defect entirely encompassed by a droplet since it implies that the interior away from the three-phase contact line matters. The analogous case is fig. 2b whereby the rough patch is entirely within the wetted area

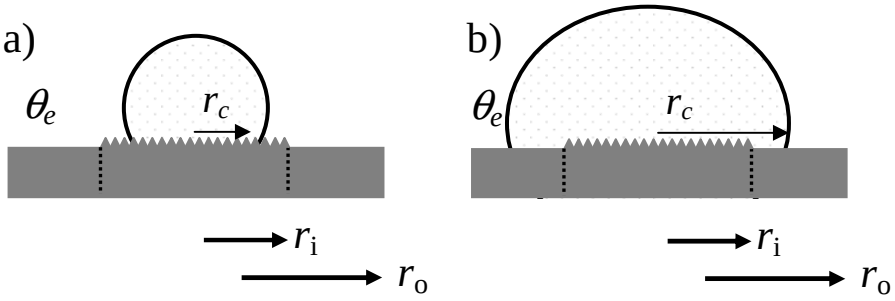

Figure 2. Droplet of contact radius r_c with its contact line on a) a rough patch of radius r_i within a smooth flat surface of radius r_o, and b) on the smooth flat surface surrounding the rough patch. All surfaces are characterized by a Young's law contact angle $\boldsymbol{\theta_e}$.

and the droplet perimeter lies entirely on the external smooth area; the rough portion of the surface does not influence the contact angle which is given by Young's law for the smooth area in the vicinity of the droplet three-phase contact line. Thus it is the surface areas in the proximity of the three-phase contact line, *x*, that matter and the appropriate definition of roughness is,

$$r(x) = \frac{\Delta A_{wetted}(x)}{\Delta A_c(x)} \tag{2}$$

where ΔA_{wetted} is a small change in wetted area that can be sampled by a three-phase contact line and $\Delta A_c = 2\pi r_c \Delta r_c$ is the planar projection of that change. More precisely, it is the first derivative in the wetted area with respect to the planar projection of area evaluated at the contact line. Thus, roughness is not an average property of the substrate or even of the substrate below the droplet, but is local to the three-phase contact line(s) where changes can occur, i.e. $r=r(x)$ where *x* is used to indicate that values are taken at the three-phase contact line. It also emphasizes that the initial state of the droplet from the deposition matters because it defines the part of the substrate surface that the three-phase contact line initially samples.

Similar arguments can be made for a surface composed of areas of two different surface chemistries (fig. 3). Provided the patchwork of different surface chemistries is entirely encompassed by the droplet (fig. 3b), only the surface chemistry of the area on which the three-phase contact line sits matters as far as the contact angle is concerned. If the three-phase contact line can sample the two different surface chemistries, the droplet contact angle, θ_{CB}, is defined by the Cassie-Baxter formula,

$$\cos\theta_{CB} = f_1 \cos\theta_1 + f_2 \cos\theta_2 \tag{3}$$

where θ_1 and θ_2 are the Young's law defined contact angles on the two surface types and the f_1 and f_2 are normally defined as the area fractions. The term area fraction could be taken to mean $f_i = A_i/(A_1+A_2)$, where A_i are the areas associated with each type of surface chemistry, but if that were to be the case we would be implying that the Cassie fractions are global properties of the substrate or of the substrate area beneath the droplet. Essentially, the hole for the syringe in fig. 1a would matter. Considering the case of fig. 3b, whereby the patchwork of the two types of surfaces is entirely encompassed within the wetted portion of the surface and the three-phase contact line sits entirely on the external area which is uniformly of one type of surface chemistry, the droplet contact angle is determined by the Young's law contact angle for that surface. Thus, it is the surface areas in the proximity of the three-phase contact line, *x*, that matter and the appropriate definition of Cassie fraction is,

$$f_i(x) = \frac{\Delta A_i(x)}{\Delta A_T(x)} \tag{4}$$

where $\Delta A_i(x)$ is the change in wetted area of type i that can be sampled by a small three-phase contact line change $\Delta A_T(x)=\Delta A_1(x)+\Delta A_2(x)$. Thus, the Cassie fractions are not average properties of the substrate or even of the substrate below the droplet, but are local to the three-phase contact line(s) where changes can occur, i.e. $f_i(x)$ where x is used to indicate that values are taken at the three-phase contact line. As with the rough surface case, it also emphasizes that the initial state of the droplet from the deposition matters because it defines the part of the substrate surface that the three-phase contact line can initially sample as it progresses towards equilibrium.

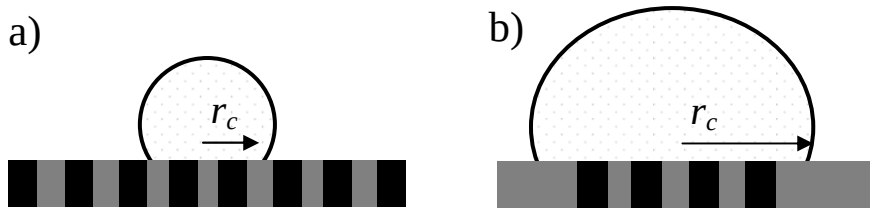

Figure 3. Cases a) and b) show two possible arrangements for droplets with their contact lines entirely on a patch possessing one type of surface chemistry. The existence of several patches with two different surface chemistries within the wetted area does not alter the contact angle, which is determined by the surface chemistry at the contact line.

The fundamental conclusion from these considerations is that the Wenzel roughness parameter, the Cassie fractions and the Young's law contact angles in the Wenzel and Cassie-Baxter formulae are local to the three-phase contact line(s) and not global properties of the substrate or of the area beneath the droplet, i.e.

$$\cos\theta_W(x) = r(x)\cos\theta_e(x) \tag{5}$$

$$\cos\theta_{CB}(x) = f_1(x)\cos\theta_1(x) + f_2(x)\cos\theta_2(x) \tag{6}$$

where the functional dependence on the location of the three-phase contact line is given by the (x) notation. When the Cassie-Baxter formula is applied to a surface consisting of a simple flat-topped post-type structure, so that $\theta_1=\theta_e$, $\theta_2=180^o$, $f_1(x)=f(x)$ and $f_2(x)=(1-f(x))$, eq. (6) can be written as,

$$\cos\theta_{CB}(x) = f(x)\cos\theta_e(x) - (1 - f(x)) \tag{7}$$

While these conclusions have been justified by comparison to a surface with a defect, it is also possible to more rigorously derive these conclusions (see ref [16]).

Arguments about wetting using surfaces visualized using a cartoon, such as fig. 3a, do not fully represent the 3-D situation in which a droplet exists. If we translate the axial symmetry for the droplet to the surface, the surface becomes a set of concentric rings with a droplet at its centre. The small change $\Delta A(x)$ that a three-phase contact line can sample is then unlikely to cover one period of the surface and unless the droplet's three-phase contact line is at the edge of a ring, the small change will only sample one type of surface. The Cassie-Baxter formula can be applied, but one of the f_i is unity and the other vanishes, resulting in a contact angle given by Young's law for that surface type. Use of the local version of the Cassie-Baxter formula (eq. 6), therefore, involves an assumption that the small change $\Delta A(x)$ is, on average, equivalent to

one period of the surface. For a droplet on a surface that does not have a symmetry in how the patches of different surface types are distributed and for a droplet much larger than the patch size and visibly demonstrating an approximately circular three-phase contact line, this might be a reasonable assumption [16] although there is no proof that these conditions alone are sufficient. Drops of comparable size to the patch sizes and ones displaying facets may not be well described by eq. (6). In addition, these considerations do not capture the full complexity that occurs between the interplay of local surface feature shape, distribution and organization, and the advancing and receding contact angles important for the design of practical liquid-shedding surfaces [26].

4. Dual Length Scales and Re-entrant Surfaces

Derivations of the results in the previous section using minimisation of changes in surface free energy for a 2-D flat-topped post-type structure have previously been presented [16]. In this section, we begin by using the same approach to consider the slightly more complicated cases of multiple length scales. Consider a post-type surface, but with the tops of the posts themselves possessing a post-type structure. The three-phase contact line may advance across one period, $\Delta A^p(x)$ of the large-scale post structure, characterised by a local Cassie fraction $f_L(x)= \Delta A^p_{Top}(x)/ (\Delta A^p_{Top}(x)+ \Delta A^p_{Bottom}(x))$ where the subscript L indicates large-scale structure, the superscript p indicates planar projections of areas and the "Top" and "Bottom" refer to the large-scale post structure.

4.1 Top-Filled Case

Focussing on the wetting of the smaller scale structure on the top of each large post, we can imagine the idealized situation in which either it is completely wetted or there is no penetration by the liquid. For the first case, corresponding to the tops being filled, the surface free energy change, $\Delta F(x)$, is,

$$\Delta F(x) = (\gamma_{SL} - \gamma_{SV}) r_S(x) f_L(x) \Delta A^p(x) + \gamma_{LV}(1 - f_L(x)) \Delta A^p(x) + \gamma_{LV} \cos\theta \Delta A^p(x) \tag{8}$$

where the γ_{ij} are the interfacial tensions and $r_S(x)$ is the local small-scale roughness at the top of the posts (indicated by the subscript S on the roughness parameter). Setting this surface free energy change to zero and using the usual definition of the Young's law contact angle, $\cos\theta_e=(\gamma_{SV} - \gamma_{SL})/\gamma_{LV}$, we find that the observed contact angle, θ_{Obs}, is given by,

$$\cos\theta_{Obs}(x) = r_S(x) f_L(x) \cos\theta_e(x) - (1 - f_L(x)) \tag{9}$$

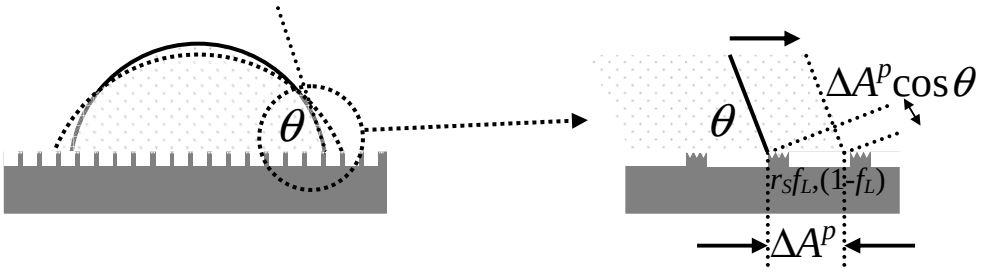

Figure 4. Changes in surface free energy as a contact line advances over a two length scale structure assuming liquid penetrates the small-scale structure at the top of posts, but does not penetrate the larger scale structure. The roughness at the top of posts is characterized by a Wenzel parameter, r_S, and the larger scale structure is described by a Cassie fraction, f_L.

4.2 Top-Empty Case

Now consider the second case, whereby the small-scale roughness at the top of each post of the larger scale structure is not penetrated by the liquid. Essentially, the top of each post in the large-scale structure corresponds to a Cassie-Baxter state rather than a Wenzel state and this is characterized by a solid fraction $f_S(x)$, where the subscript S indicates the Cassie fraction for the small-scale structure at the top of a post. The surface free energy change is then,

$$\begin{aligned}\Delta F(x) = (\gamma_{SL} - \gamma_{SV})\, f_S(x)\, f_L(x)\Delta A^p(x) + \\ \gamma_{LV}[(1 - f_L(x)) + f_L(x)(1 - f_S(x))]\Delta A^p(x) + \gamma_{LV}\cos\theta\Delta A^p(x)\end{aligned} \tag{10}$$

Setting this surface free energy change to zero and using the usual definition of the Young's law contact angle and grouping terms, we find that the observed contact angle is given by,

$$\cos\theta_{Obs}(x) = f_L(x)[f_S(x)\cos\theta_e(x) - (1 - f_S(x))] - (1 - f_L(x)) \tag{11}$$

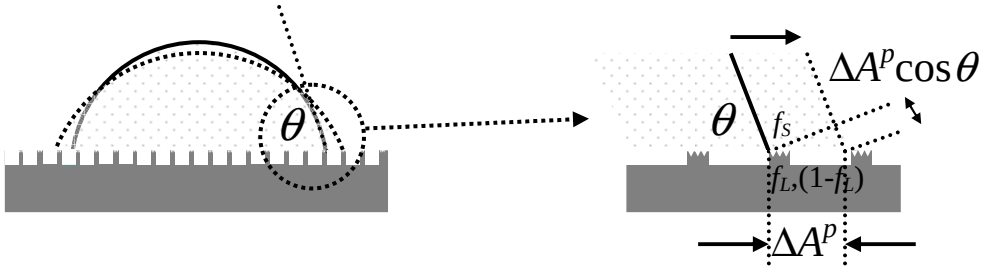

Figure 5. Changes in surface free energy as a contact line advances over a two length scale structure assuming liquid does not penetrate either the small-scale structure at the top of posts or the larger scale structure. The small-scale structure at the top of posts is described by a Cassie fraction parameter, f_S, and the larger scale structure is described by a Cassie fraction, f_L.

4.3 Transformation Formulae

Equations (9) and (11) represent different assumptions about the wetting state of the tops of the posts in the large scale structure. The formulae can be related back to the single length scale formulae (eq. 5 and eq. 7) by thinking in terms of successive transformations due to the two length scale structures. In the case of the top-filled situation, the Young's law contact angle for the smooth solid, $\theta_e(x)$, is first transformed to a local Wenzel contact angle, $\theta_W(x)$, using the local roughness factor, $r_S(x)$, existing at the top of the posts. Subsequently this local Wenzel contact angle is transformed via the Cassie-Baxter formula (eq. 7) using the solid fraction, f_L(x) for the large scale structure and the Wenzel contact angle in place of the Young's law contact angle, i.e.

$$\theta_e(x) \xrightarrow{r(x)} \theta_W(x) \xrightarrow{f_L(x)} \theta_{Obs} \tag{12}$$

In the case of the top-empty situation, the Young's law contact angle for the smooth solid, $\theta_e(x)$, is first transformed to a local Cassie-Baxter contact angle, $\theta_{CB}(x)$, using the local Cassie fraction for the small scale structure, $f_S(x)$, existing at the top of the posts. Subsequently this local Cassie-Baxter contact angle is transformed via the Cassie-Baxter formula (eq. 5) using the solid fraction, $f_L(x)$, for the large scale structure and the Cassie-Baxter contact angle from the small-scale structure in place of the Young's law contact angle, i.e.

$$\theta_e(x) \xrightarrow{f_S(x)} \theta_{CB}(x) \xrightarrow{f_L(x)} \theta_{Obs} \tag{13}$$

More complex wetting situations including roughness at the base of the large-scale structure could be considered using this approach based on minimising surface free energy changes. For example, having roughness at the base of large posts in a situation whereby tops of posts are completely wetted, but the large scale structure is a Cassie-Baxter state, would not lead to any change to eq. (12). However, if the second transformation was a Wenzel one, a roughness at the base of the large scale structure would have an effect.

4.4 Curved Features and Re-entrant Shapes

Superhydrophobic effects for curved surfaces have a long history because of the origin of the subject in the water repellency of fibers and textiles. Indeed, the original Cassie-Baxter formula was based on cylindrical shapes and used a formula similar to Eq. (9) with both a roughness factor and a Cassie-fraction [10]. One difference is that the roughness factor, which really represents the extra length of wetted area compared to a planar projection, is related to how far down a curve is wetted and this itself depends on the local Young's law contact angle. Thus, the roughness factor should be written as $r=r(x,\theta_e(x))$ indicating a dependence on the surface chemistry (and liquid since that can also result in a different Young's law contact angle) as well as the physical location. The impact of this on the wetting of spherical beads has been considered in the literature [27, 28] and is essentially an application of the transformation law given by eq. [12]. A single layer of beads is able to suspend a liquid even when the Young's law contact angle approaches 0^o. If there are multiple layers and the beads are hexagonally close-packed, a liquid will imbibe into the bead pack under capillary forces once the contact angle falls below 50.8^o, but not before unless pressure or gravity is considered as a driving force. This contact angle corresponds to the point at which the penetrating front of the liquid touches a bead from the next layer below [29]. The use of superhydrophobic ideas to describe soil, when regarded as bead packs, was first proposed in ref [27] and more recently a complete theoretical analysis based on eq. (12) and an experimental comparison have been carried out [28]. Recognition of the importance of inward (re-entrant) curves, such as observed with bead packs, in the ability of superoleophobic surfaces to suspend liquids with Young's law contact angles significantly below 90^o has recently been reported in [30].

5. Gradient Superhydrophobic Surfaces

It has long been known that on surfaces with variations in surface chemistry droplets move towards regions of lower wettability (see ref [31] and references therein). In an earlier report we suggested that lateral variation in topography to create a variation in superhydrophobicity should also generate droplet motion even when the surface chemistry was homogeneous [1, 32]. A number of reports have considered this problem experimentally with varying levels of success [32-35] and there has been at least one attempt to model this theoretically [33]. Lithographic approaches have tended to lead to droplets that are unable to move unless energy is inputted via, e.g., vibration [33], but such surfaces have been shown to be useful in inducing asymmetric rebounds from impacting droplets [37].

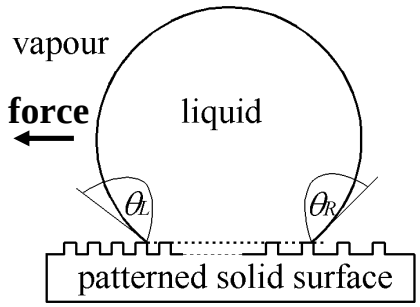

Figure 6. The concept of inducing motion by a gradient in superhydrophobicity achieved using a variation in lateral scale topography. The magnitude of the driving force, given by $\gamma_{LV}(\cos\theta_L-\cos\theta_R)$ where γ_{LV} is the liquid-vapor surface tension and θ_L and θ_R are the observed contact angles on the left and right hand sides of the droplet, must overcome contact angle hysteresis.

The basic concept of lateral gradient forces in superhydrophobicity is shown schematically in fig. 6. In this case, the horizontal spacing between features is progressively decreased across a surface so that the contact angles at the left-hand and right-hand sides of the droplet, θ_L, and θ_R, differ by a small amount. The driving force per unit length of contact line is then $\gamma_{LV}(\cos\theta_R - \cos\theta_L)$ and, assuming the surface chemistry is homogeneous, this can be written using the local form of the Cassie-Baxter equation as,

$$Force/length = \gamma_{LV}[f(x_R) - f(x_L)][1+\cos\theta_e] \tag{14}$$

Since $x_R = x_o + r_c$ and $x_L = x_o - r_c$, where x_o is the centre coordinate of the droplet in the contact plane and r_c is the contact diameter which is small, the local Cassie fractions can be expanded in terms of the gradient in Cassie fraction,

$$Force/length = 2\gamma_{LV} r_c (1+\cos\theta_e)\left(\frac{df}{dx}\right)_{x=x_o} \tag{15}$$

If we assume our droplet is a spherical cap with a small contact area we can write,

$$2r_c \approx 2R\sqrt{2f(x_o)(1+\cos\theta_e)} \tag{16}$$

where $f(x_o)$ is the average Cassie fraction between the left-hand and right-hand sides of the droplet. Hence, the force per unit length of contact line becomes,

$$Force/length = \gamma_{LV}\, 2R\sqrt{2f(x_o)}(1+\cos\theta_e)^{3/2}\left(\frac{df}{dx}\right)_{x=x_o} \tag{17}$$

For a droplet to move, this force needs to exceed the force arising from contact angle hysteresis. There are a range of possible models relating contact angle hysteresis to the Cassie fraction including one based on the Cassie-Baxter formula [38] and a more fundamental defect based model due to Joanny and de Gennes [39,40]. In the defect based model for contact angle hysteresis, the pinning force per unit length is given by the combination $-\gamma_{LV} f(x)\log_e f(x)$ and so it scales with the density of defects multiplied by a logarithmic correction. Using this with eq. (17) and rearranging, we find the following condition for the gradient in Cassie fraction for motion,

$$\left(\frac{df}{dx}\right)_{x=x_o} > \frac{-\sqrt{f(x_o)}\log_e f(x_o)}{2\sqrt{2}\,R(1+\cos\theta_e)^{3/2}} \tag{18}$$

This derivation is far from sophisticated and does not take into account shape changes around the entire contact perimeter, which can be expected to change overall constants, but it does provide an attempt to understand a number of factors preventing or initiating motion. For example, if the average Cassie fraction, $f(x_o)$, is made smaller so that the droplet is in a stronger superhydrophobic state, the gradient in Cassie fraction needed to initiate motion can be smaller. Similarly, a lower gradient is needed when the spherical radius, R, is larger. Larger volume droplets roll more easily, not because of gravity, but because the contact radius, r_c, is larger. Increasing the Young's law contact angle also reduces the need for larger gradients in the Cassie fraction.

6. An Example Gradient Surface

Considerations in the previous sections suggest self-actuated motion and definition of paths should be possible simply by varying the superhydrophobicity through topographic control and without changing surface chemistry. In this section we provide one simple experimental example of such a surface. If a widely spaced superhydrophobic surface texture is surrounded by a more narrowly spaced superhydrophobic surface texture a drop should experience a force so that it tends to roll onto the area with the more closely spaced

texture provided contact angle hysteresis can be overcome (fig. 6). The variation in lateral spacing will lead to a patterning of the effective surface free energy and hence can be used to define regions and paths on the surface [1]. A similar approach could be used with the Wenzel equation, but here we focus only on the Cassie-Baxter situation. To investigate this experimentally we modified a previously reported electrodeposition method that uses diffusion limited aggregation to create a fractally rough superhydrophobic copper surface because it can produce surfaces having an exceptionally low contact angle hysteresis [41]; stabilising even very small droplets on these surfaces is difficult. We also investigated square post based surfaces, but were unable to achieve self-actuated motion of droplets.

Figure 7. Self-initiated rolling of a water droplet on a copper surface possessing a gradient in superhydrophobicity. There is no significant overall change in average substrate height from the edge to the centre of the copper plate.

Our copper-based surface was produced using a mechanical cantilever device with two small DC motors to rotate and elevate the substrate whilst it was half immersed in a copper electroplating solution (as described in ref [41]). Samples were produced using different combinations of starting substrate material, anode material, power supply, rotation speed and elevation rate. This approach produced copper plates with a radial gradient in superhydrophobicity (θ~115^o in the centre to significantly higher than 160^o at the edge) so that drops would roll to the centre and pool, thus providing a water collection plate. This approach was highly successful with small droplets released from a hydrophobised needle of a microsyringe at the edge of the plate, always starting a self-initiated roll to the centre (fig. 7 is an image sequence showing a small droplet of water being deposited and rolling to the centre). When droplets were released so that they skirted the central part of the plate, they underwent several transits back and forth until they came to rest at the centre of the plate. We characterised our surfaces by contact profilometry and SEM imaging and established that the change in vertical height of the surface from edge to centre (a 2 cm distance) was below 25 μm (fig. 8a). The contact angle hysteresis was difficult to quantify across the sample, but to provide an estimate we tilted the surface radially such that a droplet could be stabilised at locations radially from the centre and we then measured the advancing and receding angles using a side profile view tangential to the radial direction (contact angle hysteresis is shown in fig. 8b). We also estimated the tilt angle needed to prevent a roll and this was less than 1^o at the edge of the plate.

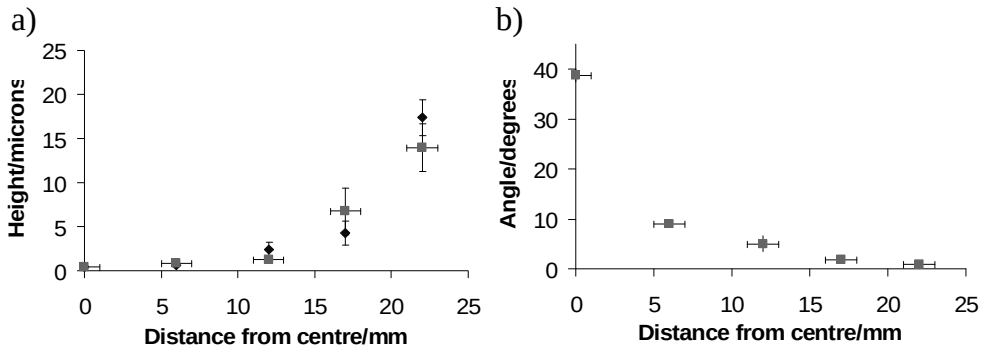

Figure 8. a) Surface topography profile measured along different radial lines, b) variations of contact angle hysteresis (*y*-axis) across sample from centre to edge (*x*-axis) estimated using radial view and tilting of table tangential to radial direction.

7. Conclusion

In this work we have emphasized that the Wenzel roughness parameter and the Cassie solid surface fractions are quantities local to the three-phase contact line and are not global parameters of the substrate or even of the substrate beneath a droplet. We have shown how the surface free energy derivations that underpin this view can provide transformation formula for multiple length scales and re-entrant surfaces based upon the Wenzel and Cassie-Baxter formulae. We have considered how the local view of the Cassie fraction can provide a condition for self-actuated droplet motion and have shown that a simple surface with a gradient in superhydrophobicity can initiate and direct droplet motion. More complex paths for use within droplet microfluidics could be designed using these principles and similar ideas could be used for droplets in Wenzel configurations and for hemi-wicking liquids.

Acknowledgements

The financial support of the UK Engineering & Physical Sciences Research Council (EPSRC) and Dstl under grant GR/S34168/01 is gratefully acknowledged.

References

1. G. McHale, N. J. Shirtcliffe and M. I. Newton, Analyst 129, 284-287 (2004).
2. G. McHale, N. J. Shirtcliffe, S. Aqil, C. C. Perry and M. I. Newton, Phys. Rev. Lett. 93, Art. 036102 (2004).
3. N. J. Shirtcliffe, G. McHale, M. I. Newton, G. Chabrol and C. C. Perry, Adv. Mater. 16, 1929-1932 (2004).
4. J. Bico, U. Thiele and D. Quéré, Colloids Surfaces A 206, 41-46 (2002).
5. D. Quéré, Physica A 313, 32-46 (2002).
6. X. J. Feng and L. Jiang, Adv. Mater. 18, 3063-3078 (2006).
7. P. Roach, N. J. Shirtcliffe and M. I. Newton, Soft Matter 4, 224-240 (2008).
8. X. M. Li, D. Reinhoudt and M. Crego-Calama, Chem. Soc. Rev. 36, 1350-1368 (2007).
9. S. H. Kim, J. Adhesion Sci. Technol. 22, 235-250 (2008).
10. A. B. D. Cassie and S. Baxter, Trans. Faraday Soc. 40, 546-551 (1944).
11. R. E. Johnson, J.r., and R. H. Dettre, in: Contact Angle, Wettability and Adhesion; Adv. Chemistry Series 43, 112-135 Amer. Chem. Soc. Washington D.C. (1964).
12. R. N. Wenzel, Ind. Eng. Chem. 28, 988-994 (1936).
13. R. N. Wenzel, J. Phys. Colloid Chem. 53, 1466-1467 (1949).
14. M. Callies and D. Quéré, Soft Matter 1, 55-61 (2005).
15. L.C. Gao and T. J. McCarthy, Langmuir 23, 3762-3765 (2007).
16. G. McHale, Langmuir 23, 8200-8205 (2007).
17. M. V. Panchagnula and S. Vedantam, Langmuir 23, 13242-13242 (2007).
18. R. B. Fair, Microfluidics Nanofluidics 3, 245-281 (2007).
19. S. Y. Teh, R. Lin, L. H. Hung and A. P. Lee, Lab on a Chip 8, 198-220 (2008).
20. D. Li and A. W. Neumann, Colloids Surfaces 43, 195-206 (1990).
21. D. Q. Li, Colloids Surfaces A 116, 1-23 (1996).
22. M. A. Rodriguez-Valverde, F. J. M. Ruiz-Cabello and M. A. Cabrerizo-Vilchez, Adv. Colloid Surface Sci. 138, 84-100 (2008).
23. C. W. Extrand, Langmuir 19, 3793-3796 (2003).
24. C. W. Extrand, Langmuir 21, 11546-11546 (2005).
25. P. G. de Gennes, Rev. Mod. Phys. 57, 827-863 (1985).
26. L. C. Gao and T. J. McCarthy, Langmuir 24, 9183-9188 (2008).
27. G. McHale, M.I. Newton and N.J. Shirtcliffe, Eur. J. Soil Sci. 56, 445-452 (2005).
28. J. Bachmann and G. McHale, Eur. J. Soil Sci. 60, 420-430 (2009).
29. N. J. Shirtcliffe, G. McHale, M. I. Newton, F. B. Pyatt and S. H. Doerr, Appl. Phys. Lett. 89, Art. 094101 (2006).

30. A. Tuteja, W. Choi, M. L. Ma, J. M. Mabry, S. A. Mazzella, G. C. Rutledge, G. H. McKinley and R. E. Cohen, Science 318, 1618-1622 (2007).
31. S. Daniel, S. Sanjoy, J. Gliem and M. K. Chaudhury, Langmuir 20, 4085-4092 (2004).
32. G. McHale, S. J. Elliott, D. L. Herbertson, N. J. Shirtcliffe and M. I. Newton, "Passive and active actuation of droplet motion", EU COST Action P21 meeting, March 29th 2007, University of Granada, Spain. (Available from http://www.naturesraincoats.com/)
33. A. Shastry, M. J. Case and K. F. Böhringer, Langmuir 22, 6161-6167 (2006).
34. J. Zhang and Y. Han, Langmuir 23, 6136-6141 (2007).
35. J. Zhang and Y. Han, Langmuir 24, 796-801 (2008).
36. C. Sun, X-W Zhao, Y-H. Han and Z-S. Ge, Thin Solid Films 516, 4059-4063 (2008).
37. M. Reyssat and D. Quéré, On «fakir» Drops, Fifth International Symposium on Contact Angle, Wettability and Adhesion, June 21st-23rd 2006, Toronto, Canada.
38. G. McHale, N. J. Shirtcliffe and M. I. Newton, Langmuir 20, 10146-10149 (2004).
39. J. F. Joanny and P. G. de Gennes, J. Chem. Phys. 81, 552-562 (1984).
40. J. F. Joanny and P. G. de Gennes, C. R. Acad. Sci. Paris Ser. II 299, 279-283 (1984).
41. N. J. Shirtcliffe, G. McHale, M. I. Newton, G. Chabrol and C. C. Perry, Langmuir 21, 937-943 (2005).